

Tuning in to Frequencies: How Global Assets Align with U.S. Put–Call Parity Residuals

Useong Shin*

May 26, 2026

JEL: G12; G13; G14

Keywords: carry gap; put–call parity; path risk; limits to arbitrage; P–Q alignment

Acknowledgments: I am grateful to Michele Azzone (Politecnico di Milano) for generously sharing OIS data, for guidance on implementing the implied-discount-factor pipeline, and for detailed feedback on earlier drafts. All remaining errors are my own.

Abstract

Put–call parity is risk-neutral at terminal payoff, but its enforcement is path-dependent and capital-using. I test whether the SPX and RUT carry gap is explained by OIS-based funding, volatility, trading-friction, and financial-condition variables, or also by residual outside-option information. Adding IEFA, IGOV, and IAU improves in-sample and leave-one-year-out fit after U.S.-centered controls. Gains survive broad-dollar neutralization, alternative blocks, PCA, residualization, and nested horizon selection. Results support reduced-form P–Q alignment: finite-capital parity enforcement reflects physical-measure investment opportunities, not payoff-level no-arbitrage failure.

*Sogang Business School, Sogang University (Seoul, Korea).
ORCID: [0009-0003-0197-9003](https://orcid.org/0009-0003-0197-9003)
Email: useong@sogang.ac.kr

1 Introduction

Put–call parity in European index options is among the cleanest no-arbitrage relations observable in real markets. Early exercise is absent, contracts are standardized, and exchange-traded futures provide a direct instrument for the forward leg. If any market should compress visible parity deviations, SPX and RUT index options should.

This clean setting makes the remaining wedge more informative. The issue is not that quoted put–call parity visibly fails. Rather, even when the price-space residual is tightly compressed, the option-implied discount factor can differ systematically from the OIS benchmark. I study this annualized difference as the carry gap: a carry-space residual associated with the implementation of parity rather than a violation of the terminal-payoff identity.

This paper builds on two earlier steps in the same framework. [Shin \(2026a\)](#) shows that the carry gap is related to a GBM path-risk term of the form $r\sigma\sqrt{\tau}$, consistent with the idea that parity enforcement is capital-using before maturity. [Shin \(2026b\)](#) shows that a prior physical-drift proxy, $\hat{\mu}$, adds explanatory power through an $r\hat{\mu}\tau$ term. Together, these results suggest that the enforcement of a risk-neutral parity relation can be exposed to physical-measure states through the implementation path, even though the terminal payoff identity itself remains risk-neutral.

The present paper asks whether this physical-measure component is better viewed as a narrow own-index drift effect or as part of a broader outside-option state. If capital is tied to parity enforcement, it cannot be deployed elsewhere. The relevant opportunity cost may therefore be only partly summarized by OIS rates. It may also reflect low-frequency investment opportunities available to the finite-capital arbitrageurs who enforce parity. I test this idea by adding a parsimonious 3ETF block—IEFA, IGOV, and IAU—to the OIS-based baseline. These assets proxy for developed ex-U.S. equity, international sovereign bonds, and gold, respectively. Each component is constructed from a prior rolling OLS slope of the log price path, using only information available through $t - 1$.

The 3ETF block substantially improves the baseline in both markets. In-sample R^2 rises from 0.312 to 0.402 in SPX and from 0.281 to 0.361 in RUT. Leave-one-year-out pooled out-of-sample R^2 rises from 0.221 to 0.379 in SPX and from 0.171 to 0.318 in RUT. The result is not confined to a single holdout year and survives broad-dollar neutralization, PCA and residualization tests, alternative asset blocks, and nested horizon selection. The improvement is therefore difficult to interpret as a simple in-sample fit gain or a disguised U.S.-dollar factor.

The absorption pattern is also informative. Once the 3ETF block is included, the own-index $\hat{\mu}$ proxy adds little incremental explanatory power. Thus, the drift proxy is not rejected; rather, it appears to be a scalar projection of a broader physical-measure investment-

opportunity state. The evidence should be read as reduced-form P–Q alignment, not as a structural P-to-Q transmission model. Put–call parity remains a terminal-payoff identity. The claim is narrower: a carry-space residual constructed from option-implied and OIS discount factors can align with physical-measure outside-option components because the risk-neutral parity relation is enforced by finite-capital intermediaries.

The rest of the paper proceeds as follows. Section 2 reviews the related literature. Section 3 motivates the outside-option channel. Section 4 describes the carry gap, the baseline specification, and the asset-return-based GBM terms. Section 5 derives the 3ETF specification. Section 6 reports the main empirical results. Section 7 compares the 3ETF specification with the drift-extended specification. Section 8 presents robustness checks. Section 9 discusses interpretation and limitations. Section 10 concludes. Appendix A provides data-processing and implementation details.

2 Related Literature

This paper connects three literatures: put–call parity and option-implied discounting, limits to arbitrage and intermediary capital, and the relation between risk-neutral objects and physical-measure state variables. It also directly extends [Shin \(2026a\)](#) and [Shin \(2026b\)](#). The common theme is that no-arbitrage relations are exact at the terminal-payoff level, but their enforcement in actual markets can be path-dependent, capital-using, and exposed to physical-measure investment opportunities.

2.1 Put–Call Parity and Implied Discounting

Put–call parity has been a basic no-arbitrage relation in option pricing since [Stoll \(1969\)](#). The empirical literature asks whether observed parity deviations represent genuine arbitrage opportunities or instead reflect transaction costs, short-sale constraints, execution frictions, and market microstructure noise ([Gould and Galai, 1974](#); [Klemkosky and Resnick, 1979](#); [Ackert and Tian, 2001](#)). The common implication is that observed price-space deviations should not be interpreted mechanically as risk-free arbitrage opportunities.

I study a different object. Using the option-implied discount-factor procedure of [Azzone and Baviera \(2021\)](#), I estimate discount factors from SPX and RUT option cross-sections and compare them with OIS discount factors. This yields the carry gap, an annualized carry-space wedge. The question is therefore not whether quoted put–call parity visibly fails, but which state variables align with the wedge that remains after visible parity deviations have largely been compressed.

2.2 Limits to Arbitrage after Visible Parity Is Closed

The interpretation builds on the limits-to-arbitrage literature. Since [Shleifer and Vishny \(1997\)](#), this literature has emphasized that arbitrage is performed by finite-capital intermediaries who face funding constraints, margin requirements, interim losses, and liquidation risk ([Gromb and Vayanos, 2002](#); [Brunnermeier and Pedersen, 2009](#); [Mitchell and Pulvino, 2012](#)). In options markets, [Ofek et al. \(2004\)](#) show that short-sale constraints and limits to arbitrage can be linked to put–call parity deviations.

My setting is deliberately different from the standard short-sale-constraint environment. Much of the existing evidence studies cases in which visible price-space deviations remain open because arbitrage is directly impeded. Here, the visible put–call parity residual is already tightly compressed in liquid European index-option markets. The question is why a systematic carry-space wedge remains after the obvious price-space arbitrage has largely been closed.

This view is also consistent with work linking intermediary capital to law-of-one-price deviations ([Gârleanu and Pedersen, 2011](#); [He and Krishnamurthy, 2013](#); [Adrian et al., 2014](#); [He et al., 2017](#)). It is close in spirit to the CIP evidence in [Du et al. \(2018\)](#): enforcing no-arbitrage relations uses balance-sheet capacity, capital, and margin, and the marginal cost of that enforcement varies with market conditions. The contribution here is to apply this logic to a clean parity setting and to ask whether the remaining carry-space wedge is aligned with outside investment opportunities faced by finite-capital arbitrageurs.

2.3 Risk-Neutral Objects and Physical-Measure States

This paper also relates to work connecting option-implied, risk-neutral objects to physical-measure information. [Bollerslev et al. \(2009\)](#), [Ross \(2015\)](#), and [Martin \(2017\)](#) show that option-implied Q -measure objects can contain information about variance risk premia, physical probabilities, or expected returns.

My direction is complementary. I do not recover physical probabilities from option prices, and I do not identify a structural mapping from physical returns to risk-neutral prices. Instead, I ask whether a Q -measure carry-space residual is empirically aligned with P -measure outside-option proxies because the parity relation is enforced by finite-capital intermediaries. This question is related to investment-opportunity-state models such as [Merton \(1973\)](#)'s ICAPM, [Ross \(1976\)](#)'s APT, and multi-factor asset-pricing frameworks ([Campbell, 1993](#); [Campbell and Vuolteenaho, 2004](#); [Chen et al., 1986](#); [Fama and French, 1993](#); [Petkova, 2006](#)). The exercise is not a structural ICAPM or APT test; it is a reduced-form test of whether the opportunity cost of parity-enforcement capital is aligned with multiple physical-measure

state variables.

2.4 Direct Antecedents

This paper directly extends [Shin \(2026a\)](#) and [Shin \(2026b\)](#). [Shin \(2026a\)](#) documents the carry gap and shows that OIS-based GBM path-risk terms, trading frictions, and financial conditions explain a meaningful part of its variation. The key reduced-form object is an $r\sigma\sqrt{\tau}$ implementation-risk term.

[Shin \(2026b\)](#) extends the framework by preserving physical drift in the support-capital logic. Since the true physical drift μ is unobserved, that paper uses a prior rolling trend in the own-index total return as a proxy $\hat{\mu}$, and shows that an $r\hat{\mu}\tau$ term adds explanatory power for the carry gap. The present paper asks whether this own-index drift proxy is an independent state variable or a scalar projection of a broader outside-option state. To test this, I introduce a 3ETF block consisting of IEFA, IGOV, and IAU, and compare the baseline, drift, 3ETF, and 3ETF+drift specifications.

3 Motivation for the Asset Extension

This section motivates the extension from the OIS-based baseline to asset-return components. The key idea is simple. Capital tied to parity enforcement cannot be deployed elsewhere. Even if the terminal payoff of put–call parity is fixed, the enforcing strategy must be carried through variation margin, funding needs, trading frictions, and finite-capital constraints. The carry gap may therefore respond not only to OIS rates, but also to the outside investment opportunities forgone by arbitrageurs.

Consider a finite-capital arbitrageur, Bob. Bob observes a small put–call parity wedge in the SPX or RUT options market and enters a parity-enforcement position combining a synthetic forward and a futures leg. At the terminal-payoff level, the trade is nearly locked. Before maturity, however, Bob must absorb daily mark-to-market gains and losses and meet variation-margin calls. If supporting the trade requires reducing other risky or liquid positions, Bob forgoes the expected return, liquidity service, or balance-sheet capacity those positions would have provided. Thus, even when the terminal payoff is fixed, the implementation path has an opportunity cost.

From this perspective, restricting the opportunity-cost component of the baseline GBM term to OIS rates may be too narrow. OIS rates are a natural benchmark for risk-free funding costs, but the actual capital-allocation problem of a finite-capital arbitrageur is broader. Bob compares harvesting the parity wedge with deploying the same capital elsewhere. The

shadow cost of parity-enforcement capital may therefore reflect low-frequency outside-option states as well as risk-free rates.

The asset extension implements this idea inside the GBM structure. The baseline specification can be written conceptually as

$$\text{GBM term} = \text{path-risk scale} \times \text{opportunity-cost component}.$$

In the baseline, the opportunity-cost component is proxied by OIS rates. In the 3ETF extension, I expand this component using low-frequency return components of global equity, sovereign bonds, and gold. The 3ETF block is therefore not a generic set of added predictors. It is a reduced-form proxy for the outside-option set faced by a finite-capital arbitrageur.

This interpretation also connects to the drift extension. [Shin \(2026b\)](#) shows that an own-index rolling drift proxy, $\hat{\mu}$, adds explanatory power for the carry gap through an $r\hat{\mu}\tau$ term. I ask whether this proxy is an independent scalar primitive, or instead a compressed proxy for a broader physical-measure state that partly overlaps with U.S. financial conditions and partly extends beyond them. To examine this, I compare the baseline, drift, 3ETF, and 3ETF+drift specifications.

The empirical predictions are direct. If the carry gap is an OIS-contained wedge, adding asset-return components should produce only limited gains over the baseline. If the carry gap is aligned with outside-option states, low-frequency components from equities, bonds, and gold should add explanatory power. If the 3ETF block absorbs the information in the own-index $\hat{\mu}$ proxy, then the drift effect is better interpreted as a scalar projection of a broader residual opportunity-cost state rather than as an independent primitive.

4 Data and Methodology

This section summarizes the carry-gap measure, the OIS-based baseline, the asset-return GBM terms, and the comparison models. [Appendix A](#) provides implementation details on data cleaning, option-implied discount-factor identification, ETF slope construction, broad-dollar adjustment, HAC inference, and leave-one-year-out evaluation.

4.1 Carry Gap

I study European-style SPX and RUT index options using minute-level NBBO quotes from ThetaData. The sample runs from January 4, 2016 to October 31, 2025, the period over which the OIS data used in the baseline are available. Because both markets use European-style index options, early-exercise premia do not directly affect the put–call-parity-based

identification of discount factors.

Following [Azzone and Baviera \(2021\)](#), I estimate the option-implied discount factor $\hat{B}_t(T)$ from synthetic-forward relations and compare it with the OIS discount factor $D_t^{\text{OIS}}(T)$. Let $\tau_t(T) = T - t$. The carry gap is

$$CG_t(T) = \frac{1}{\tau_t(T)} \log \left(\frac{D_t^{\text{OIS}}(T)}{\hat{B}_t(T)} \right), \quad (1)$$

and I use the basis-point version

$$CG_t^{bp}(T) = 10^4 \cdot CG_t(T). \quad (2)$$

The regression outcome, $CG_{i,t}^{bp}$, is the cleaned daily market-level carry gap for market $i \in \{\text{SPX}, \text{RUT}\}$.

4.2 Baseline and Asset-Return GBM Terms

The baseline is an OIS-based GBM path-risk specification:

$$CG_{i,t}^{bp} = \alpha_i + \phi_{1,i} GBM_{i,t}^{\text{OIS},1Y} + \phi_{10,i} GBM_{i,t}^{\text{OIS},10Y} + \beta_i \frac{BA_{i,t}^{med}}{\tau_{i,t}} + \gamma_i NFCI_t + \varepsilon_{i,t}. \quad (3)$$

The two OIS GBM terms use the one-year and ten-year OIS rates as opportunity-cost components. The variable $BA_{i,t}^{med}/\tau_{i,t}$ captures ATM option-market trading frictions, and $NFCI_t$ is the Chicago Fed National Financial Conditions Index.

Conceptually,

$$\text{GBM term} = \text{path-risk scale} \times \text{opportunity-cost component}.$$

The asset extension keeps this structure but replaces part of the opportunity-cost component with low-frequency outside-option return proxies. For asset a and lookback window n , define

$$GBM_{i,t}^{a,n} = 10^4 \cdot b_{a,t}^{(n)} \cdot \frac{2}{3} \cdot \frac{Vol_{i,t}}{100} \cdot \sqrt{\frac{2\tau_{i,t}}{\pi}}, \quad (4)$$

where $b_{a,t}^{(n)}$ is the prior n -day rolling OLS slope of ETF a 's log price path, computed using information through $t - 1$. The volatility input $Vol_{i,t}$ is VIX for SPX and RVX for RUT. Thus, the asset-return term places an outside-option return proxy in the slot occupied by the OIS rate in the baseline GBM term.

4.3 Comparison Models and Evaluation

I compare four specifications. The baseline includes the OIS 1Y and OIS 10Y GBM terms. The drift specification adds the own-index rolling drift proxy $\hat{\mu}$, since the true physical drift μ is unobserved. The 3ETF specification keeps OIS 1Y, drops OIS 10Y, and adds IEFA, IGOV, and IAU GBM terms. The 3ETF+drift specification adds the own-index $\hat{\mu}$ proxy to the 3ETF model.

The comparison asks two questions. First, do outside-option components improve on the OIS-only baseline? Second, does the own-index $\hat{\mu}$ proxy retain independent explanatory power once the 3ETF block is included? If 3ETF+drift adds little to 3ETF, the drift proxy is better interpreted as a scalar projection of the broader residual opportunity-cost state.

All regressions are estimated separately for SPX and RUT. Coefficient inference uses date-based HAC (Newey–West) standard errors. Out-of-sample performance is evaluated by leave-one-year-out validation.

5 Selecting the 3ETF Block

This section explains how I select the 3ETF specification. The exercise is a restricted asset-allocation scan, not an unrestricted predictor search. I begin with standard outside-option categories—equities, bonds, and gold—and vary the regional equity and bond components across U.S., developed ex-U.S., and emerging-market blocks.

5.1 Candidate Assets

I first compute the incremental R^2 over the OIS-based baseline for each candidate ETF across lookback horizons. The candidate set contains ten ETFs covering major asset-allocation categories.¹ For each ETF and lookback window, I convert the prior log-price slope into the asset-return GBM term in Section 4 and measure the fit gain relative to the baseline.

¹VTI (U.S. equity), IEFA (developed ex-U.S. equity), IEMG (emerging-market equity), BND (U.S. aggregate bond), SCHP (U.S. inflation-linked bond), IGOV (developed ex-U.S. sovereign bond, FX-unhedged), EBND (emerging-market sovereign bond, FX-unhedged), IAU (gold), VNQ (U.S. REITs), and VNQI (ex-U.S. REITs).

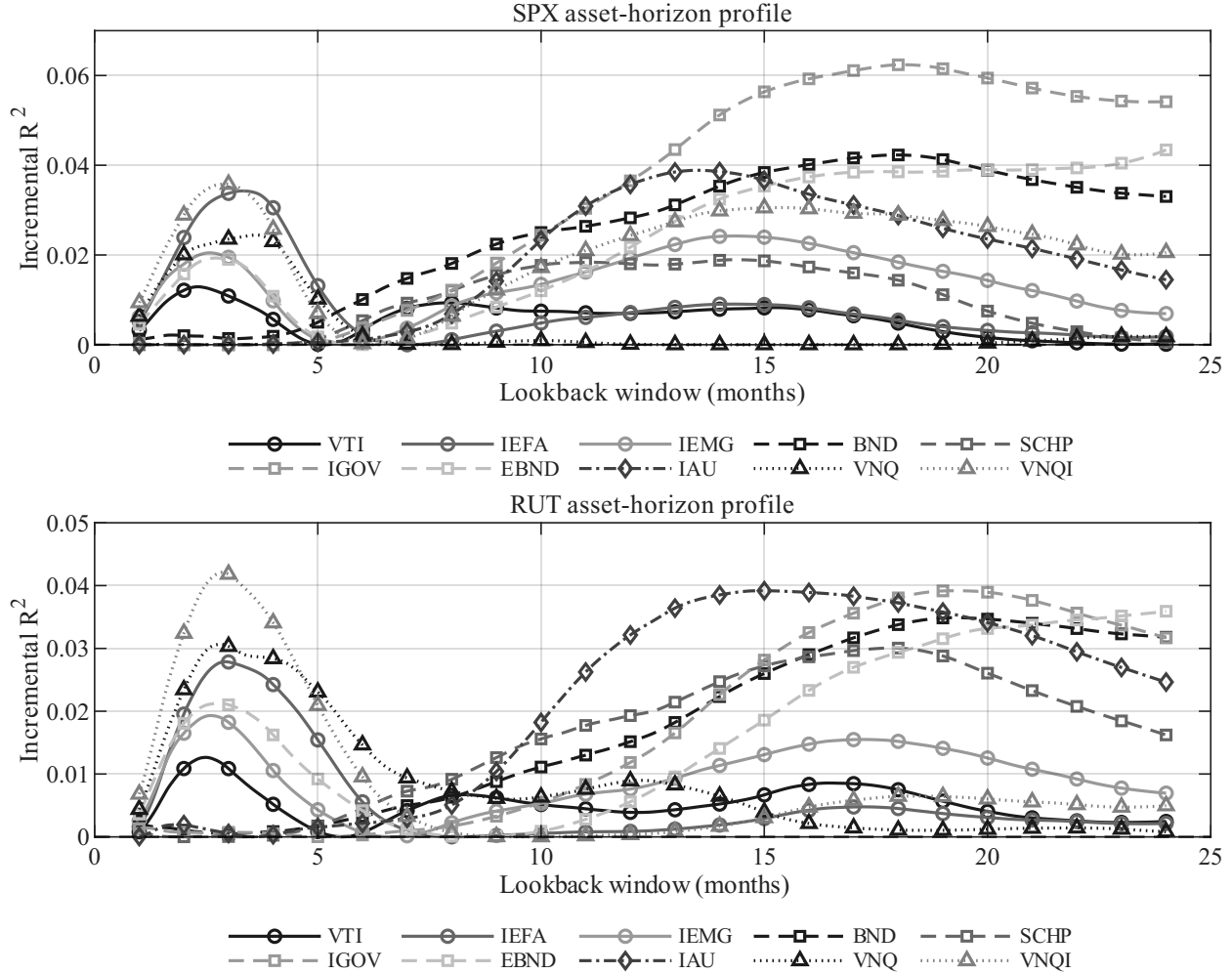


Figure 5.1: Incremental R^2 by lookback horizon for ETFs representing major asset classes. The upper panel reports SPX results; the lower panel reports RUT results.

Figure 5.1 shows that the useful outside-option information is not concentrated at a single frequency. IEFA is informative at relatively short horizons, IGOV at much longer horizons, and IAU at medium-to-long horizons. The peaks are also surrounded by broad high- R^2 plateaus, so the selected lookbacks should be read as representative horizon bands rather than pointwise optimized constants.

5.2 Selected Horizons

Following the asset-allocation taxonomy, I compare three blocks: a U.S.-centered block (VTI, BND, IAU), a developed ex-U.S. block (IEFA, IGOV, IAU), and an emerging-market block (IEMG, EBND, IAU). All three improve on the OIS-only baseline. The developed ex-U.S. block performs best overall, so I use IEFA, IGOV, and IAU as the main 3ETF

specification. Section 8 revisits the other two blocks as alternative-asset robustness checks.

The final lookback windows are 70 trading days for IEFA, 441 trading days for IGOV, and 315 trading days for IAU. IEFA represents a fast developed ex-U.S. equity component, IGOV a slow international sovereign-bond component, and IAU an intermediate gold component.

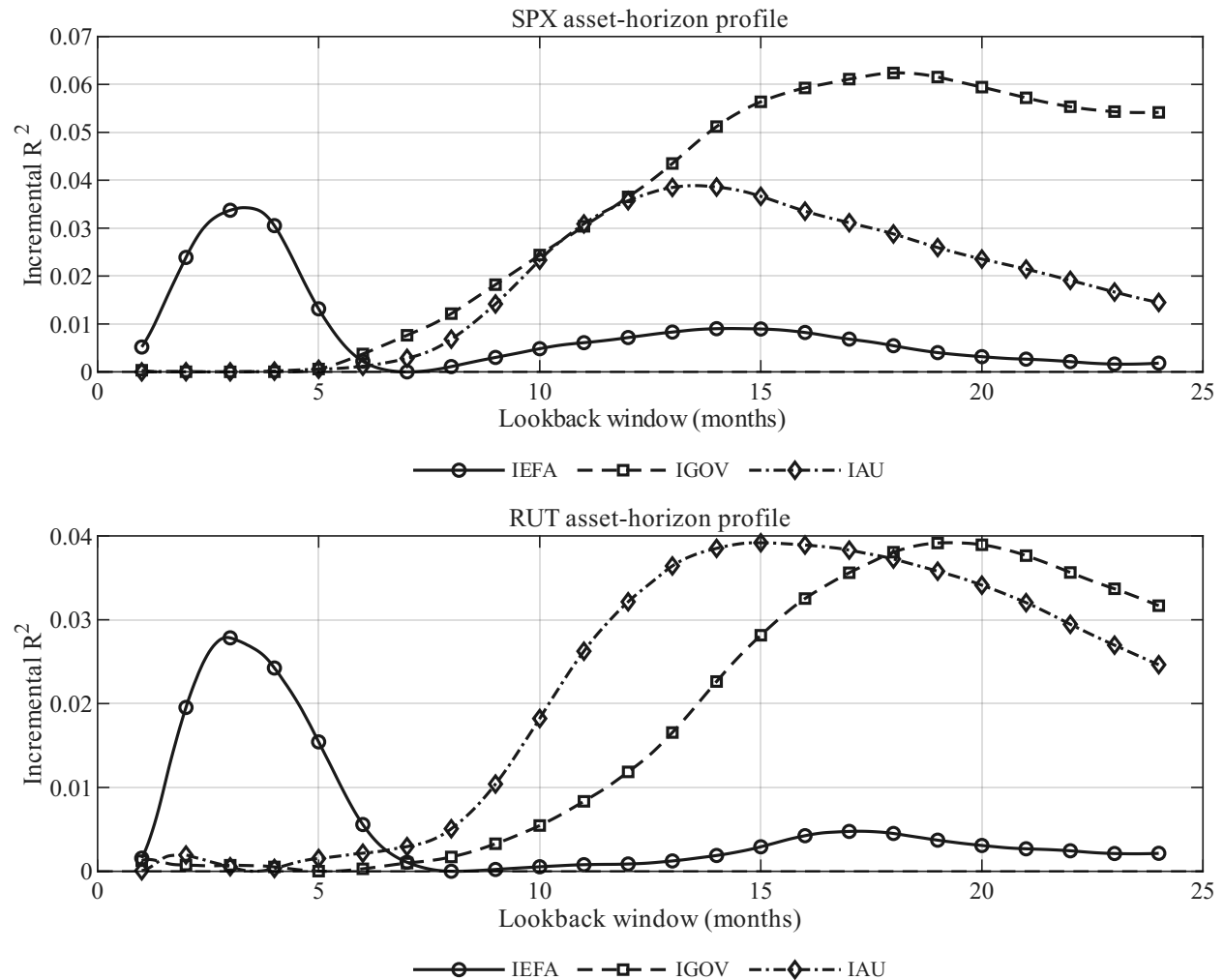


Figure 5.2: Incremental R^2 by lookback horizon for the three selected ETFs. The upper panel reports SPX results; the lower panel reports RUT results.

Figure 5.2 isolates the three retained components. The selected ETFs line up with different horizon bands in both SPX and RUT: IEFA at short horizons, IGOV at long horizons, and IAU between them. This frequency heterogeneity is the reason the final block uses three assets rather than a single outside-option proxy.

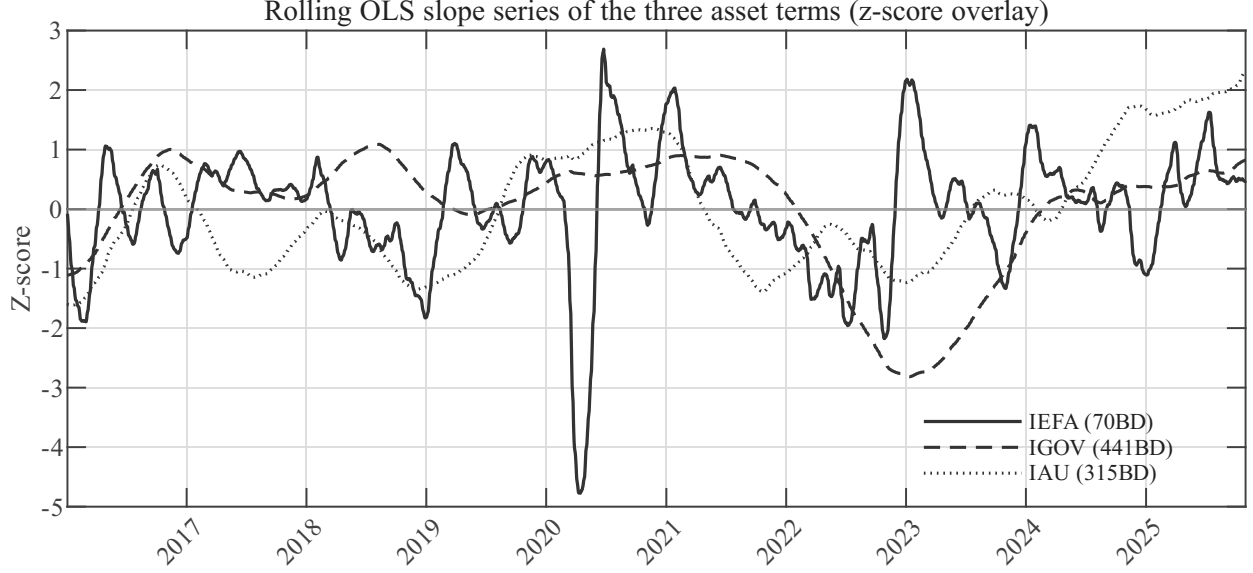


Figure 5.3: OLS slope series of the three selected ETFs. Each series is the log OLS slope under the lookback window used in the main specification (IEFA: 70 days, IGOV: 441 days, IAU: 315 days), standardized as a z -score.

Figure 5.3 shows the same point in the time-series domain. IEFA moves relatively quickly, IGOV moves slowly, and IAU lies between them. The 3ETF block therefore combines outside-option components with distinct low-frequency speeds rather than stacking parallel versions of the same signal. Section 8 tests this interpretation directly using PCA and residualization.

5.3 Final Specification

The final 3ETF regression keeps the OIS 1Y GBM term, drops the OIS 10Y GBM term, and adds the IEFA, IGOV, and IAU GBM terms. The exclusion of OIS 10Y is empirical: IGOV overlaps with the long-horizon opportunity-cost variation previously captured by OIS 10Y, and including both terms destabilizes the coefficient structure with little gain in fit. The selected block therefore replaces the long-horizon OIS component rather than being stacked mechanically on top of the full baseline.

For market $i \in \{\text{SPX}, \text{RUT}\}$, the final regression is

$$\begin{aligned}
 CG_{i,t}^{bp} = & \alpha_i + \phi_{1,i} GBM_{i,t}^{\text{OIS},1Y} \\
 & + \theta_{E,i} GBM_{i,t}^{\text{IEFA},70} + \theta_{G,i} GBM_{i,t}^{\text{IGOV},441} + \theta_{A,i} GBM_{i,t}^{\text{IAU},315} \\
 & + \beta_i \frac{BA_{i,t}^{med}}{\tau_{i,t}} + \gamma_i NFCI_t + \varepsilon_{i,t}.
 \end{aligned} \tag{5}$$

The specification layers a restricted outside-option block on top of the short-horizon OIS opportunity-cost component. The next section evaluates how much this structure improves in-sample and out-of-sample fit relative to the OIS-based baseline.

6 Empirical Results

This section compares the OIS-based baseline with the 3ETF asset-return extension. The baseline includes OIS 1Y and OIS 10Y GBM path-risk terms. The 3ETF specification keeps OIS 1Y, drops OIS 10Y, and adds IEFA, IGOV, and IAU GBM terms. The central question is whether the outside-option block improves fit even after the long-horizon OIS component is removed.

6.1 In-Sample Performance

Table 6.1: In-sample performance: baseline versus 3ETF specification

Market	R^2 (baseline)	R^2 (3ETF)	ΔR^2	ΔRMSE (bp)	ΔMAE (bp)
SPX	0.312	0.402	0.090	-0.893	-0.942
RUT	0.281	0.361	0.080	-0.804	-0.687

Table 6.1 shows that the 3ETF specification improves the maturity-pooled fit in both markets. In SPX, R^2 rises from 0.312 to 0.402. In RUT, it rises from 0.281 to 0.361. RMSE and MAE decline in both markets.

The gain is not a mechanical consequence of stacking more predictors on the full baseline. The 3ETF specification removes the OIS 10Y GBM term and still improves fit. This suggests that part of the low-frequency carry-gap variation previously assigned to long-horizon OIS rates is better captured by residual asset-return components conditional on the U.S.-centered baseline.

Maturity-pooled daily series: baseline vs with ETFs

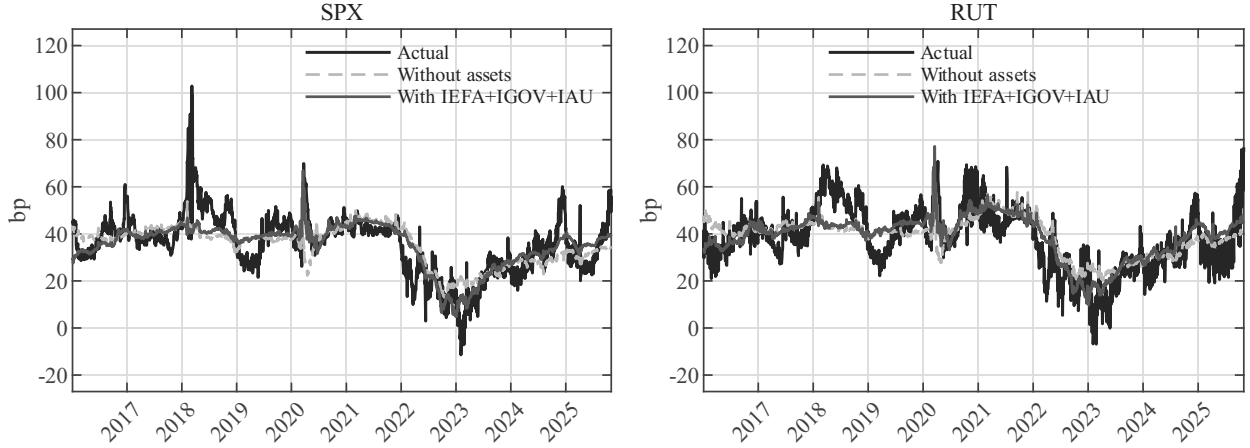


Figure 6.1: Maturity-pooled daily fit: baseline versus 3ETF specification

Figure 6.1 gives the corresponding time-series view. In both markets, the 3ETF fitted value tracks low-frequency movements in the carry gap more closely than the baseline, especially around the post-2020 decline and the 2024–2025 recovery. The improvement is therefore visible not only in summary fit statistics, but also along the daily carry-gap path.

6.2 Performance by Maturity Bin

Table 6.2: In-sample performance by maturity bin: baseline versus 3ETF specification

Market	Maturity bin	R^2 (baseline)	R^2 (3ETF)	ΔR^2	$\Delta RMSE$ (bp)	ΔMAE (bp)
SPX	1–2m	0.096	0.136	0.039	-0.502	-0.577
SPX	2–3m	0.184	0.257	0.073	-0.815	-0.676
SPX	3–5m	0.283	0.401	0.118	-1.165	-0.866
SPX	5–7m	0.373	0.532	0.159	-1.555	-1.018
SPX	7–10m	0.472	0.630	0.157	-1.590	-1.101
SPX	10–14m	0.525	0.621	0.096	-0.884	-0.905
SPX	14–21m	0.306	0.359	0.054	-0.508	-1.118
SPX	21m+	0.182	0.195	0.013	-0.106	-1.209
RUT	1–2m	0.112	0.164	0.052	-0.665	-0.537
RUT	2–3m	0.205	0.304	0.099	-1.007	-0.633
RUT	3–5m	0.254	0.370	0.116	-1.047	-0.761
RUT	5–7m	0.231	0.429	0.198	-1.737	-1.352
RUT	7–10m	0.284	0.461	0.177	-1.573	-1.149
RUT	10–14m	0.472	0.550	0.077	-0.801	-0.848
RUT	14–21m	0.482	0.517	0.035	-0.347	-0.359
RUT	21m+	0.413	0.256	-0.157	1.348	0.755

Table 6.2 shows that the 3ETF gain is strongest at intermediate maturities. In SPX, ΔR^2 reaches 0.159 in the 5–7 month bin and 0.157 in the 7–10 month bin. In RUT, the corresponding gains are 0.198 and 0.177. The pattern is consistent with the interpretation that the outside-option channel is most visible where the enforcement path is long enough for carry and margin costs to accumulate, but not so long that additional slow-moving maturity-specific components dominate.

The far long end is more mixed. SPX still improves slightly at 21m+, but RUT deteriorates in that bin. I therefore interpret the maturity-bin evidence as supporting an intermediate-horizon outside-option channel, not as showing that the 3ETF block uniformly dominates the baseline at every maturity.

6.3 Out-of-Sample Performance

The out-of-sample exercise should be read as a stability test, not as a real-time forecasting experiment. The sample spans only nine years and ten months, which makes a conventional expanding-window design unattractive: early training windows would be short and regime-specific, especially for low-frequency asset components. Leave-one-year-out validation instead uses the sample symmetrically by allowing every calendar year to serve once as a holdout period. Because each holdout model is estimated on all remaining years, the exercise is not a trading forecast. Its purpose is narrower: to test whether the 3ETF relation is concentrated in a small number of calendar years, or whether it survives the exclusion of any single year.

Table 6.3: LOYO out-of-sample performance: baseline versus 3ETF specification

Market	Specification	Mean R^2	Median R^2	Pooled R^2	Mean RMSE (bp)	Mean correlation
SPX	Baseline	0.059	0.130	0.221	13.95	0.205
SPX	3ETF	0.288	0.195	0.379	12.37	0.373
RUT	Baseline	0.075	0.108	0.171	15.07	0.243
RUT	3ETF	0.237	0.211	0.318	13.83	0.356

Table 6.3 reports the LOYO summary. The 3ETF specification outperforms the baseline in both markets. In SPX, pooled OOS R^2 rises from 0.221 to 0.379. In RUT, pooled OOS R^2 rises from 0.171 to 0.318. Mean OOS R^2 and mean correlation also increase, while mean RMSE declines in both markets. The improvement therefore is not limited to in-sample fit; the asset-return block continues to explain carry-gap variation when each calendar year is excluded from estimation in turn.

LOYO OOS R^2 : baseline vs with ETFs

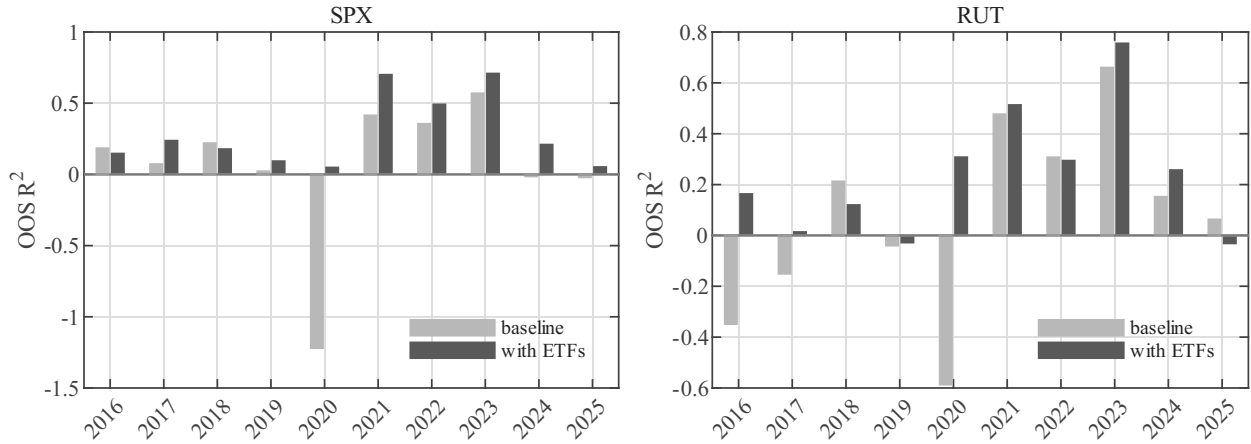


Figure 6.2: Year-by-year LOYO out-of-sample performance: baseline versus 3ETF specification

Figure 6.2 compares OOS R^2 by holdout year. The improvement is not driven by a single calendar year. The 3ETF model beats the baseline in 8 out of 10 SPX holdouts and 7 out of 10 RUT holdouts. The largest repair occurs in 2020, when the baseline fit breaks down sharply. In SPX, OOS R^2 moves from -1.221 under the baseline to 0.050 under the 3ETF specification. In RUT, it moves from -0.587 to 0.308 . Thus, the 3ETF block helps most when the OIS-only baseline loses its level calibration.

Table 6.4: Year-by-year LOYO out-of-sample performance: SPX

Holdout year	Baseline			3ETF		
	R^2	RMSE (bp)	Corr.	R^2	RMSE (bp)	Corr.
2016	0.185	8.970	0.194	0.148	9.173	0.363
2017	0.074	10.069	0.226	0.238	9.133	0.394
2018	0.221	26.304	0.259	0.179	26.997	0.181
2019	0.023	8.934	-0.011	0.094	8.604	0.271
2020	-1.221	18.423	-0.294	0.050	12.048	0.416
2021	0.416	7.600	0.064	0.701	5.436	0.092
2022	0.357	16.040	0.347	0.493	14.238	0.285
2023	0.571	15.725	0.438	0.710	12.932	0.509
2024	-0.016	15.428	0.589	0.211	13.599	0.751
2025	-0.022	11.980	0.242	0.053	11.529	0.473
Mean	0.059	13.947	0.205	0.288	12.369	0.373
Median	0.130			0.195		
Pooled	0.221			0.379		

Table 6.5: Year-by-year LOYO out-of-sample performance: RUT

Holdout year	Baseline			3ETF		
	R^2	RMSE (bp)	Corr.	R^2	RMSE (bp)	Corr.
2016	-0.350	12.787	0.069	0.164	10.066	0.267
2017	-0.152	10.498	0.142	0.014	9.712	0.361
2018	0.213	18.830	0.121	0.120	19.911	0.203
2019	-0.041	11.088	-0.007	-0.029	11.025	0.422
2020	-0.587	22.437	0.102	0.308	14.809	0.437
2021	0.477	12.368	0.431	0.514	11.930	0.353
2022	0.308	16.619	0.368	0.295	16.776	0.238
2023	0.661	13.922	0.354	0.756	11.810	0.458
2024	0.153	14.005	0.598	0.258	13.110	0.486
2025	0.064	18.193	0.248	-0.032	19.101	0.335
Mean	0.075	15.075	0.243	0.237	13.825	0.356
Median	0.108			0.211		
Pooled	0.171			0.318		

Tables 6.4 and 6.5 report the year-by-year results. In SPX, the 3ETF specification has a higher OOS R^2 in all holdout years except 2016 and 2018. In RUT, it outperforms the baseline except in 2018, 2022, and 2025. In 2019, both RUT specifications have negative OOS R^2 , but the loss is smaller under the 3ETF specification.

The main lesson is that the 3ETF block improves average fit and also mitigates some of the baseline’s worst failures. The evidence is not uniform across every year: some holdouts still favor the baseline, and RUT 2025 remains negative under the 3ETF specification. I therefore do not interpret the 3ETF model as a complete forecasting model. The more appropriate interpretation is that the 3ETF block captures a low-frequency outside-option component missed by the OIS-only baseline, improving overall out-of-sample stability and stress-year calibration.

6.4 Coefficient Structure

This subsection examines the coefficient structure behind the fit gains. The full-sample HAC estimates show signs, magnitudes, and statistical significance. The LOYO training estimates show whether the coefficients used in the out-of-sample exercise are stable across holdout folds.

Table 6.6: In-sample coefficients: baseline versus 3ETF specification, HAC inference

Variable	SPX baseline	SPX 3ETF	RUT baseline	RUT 3ETF
Intercept	23.134*** (5.713)	19.551*** (4.434)	24.577*** (5.407)	13.945*** (3.805)
$GBM^{OIS,1Y}$	-0.548*** (0.170)	-0.128*** (0.047)	-0.555*** (0.124)	-0.109*** (0.031)
$GBM^{OIS,10Y}$	0.411** (0.172)	–	0.541*** (0.130)	–
$GBM^{IEFA,70}$	–	-0.00838*** (0.00146)	–	-0.00749*** (0.00111)
$GBM^{IGOV,441}$	–	0.0401** (0.0160)	–	0.00830 (0.0130)
$GBM^{IAU,315}$	–	0.0142** (0.00657)	–	0.0232*** (0.00486)
BA^{med}/τ	0.256*** (0.0635)	0.195*** (0.0673)	0.130*** (0.0225)	0.137*** (0.0256)
$NFCI$	-25.839** (10.359)	-34.798*** (7.712)	-23.961** (10.013)	-47.980*** (6.733)
R^2	0.3124	0.4023	0.2809	0.3613
Adj. R^2	0.3123	0.4022	0.2807	0.3611
RMSE (bp)	13.199	12.306	13.951	13.148
MAE (bp)	8.682	7.740	10.103	9.417

Notes: Parentheses report date-based HAC (Newey–West) standard errors with a 21-trading-day lag. ***, **, and * denote significance at the 1%, 5%, and 10% levels. The baseline includes both OIS 1Y and OIS 10Y GBM terms. The 3ETF specification drops the OIS 10Y term and includes GBM terms based on IEFA, IGOV, and IAU.

Table 6.6 shows that the 3ETF specification changes the composition of the opportunity-cost block without eliminating the OIS channel. In the baseline, the OIS 1Y term is negative and the OIS 10Y term is positive in both markets. In the 3ETF specification, OIS 10Y is removed, but OIS 1Y remains negative and statistically significant. Thus, the short-horizon OIS component survives the asset extension; what changes is the representation of the slower opportunity-cost component.

The asset coefficients have a clear conditional pattern. IEFA enters negatively and is strongly significant in both SPX and RUT. Conditional on OIS rates, trading frictions, and financial conditions, a stronger developed ex-U.S. equity component is associated with a lower carry gap. This is consistent with IEFA capturing a global risk-bearing or capital-availability state: when that state is stronger, the carry-space wedge is smaller.

IAU enters with the opposite sign. The gold component is positive and statistically significant in both markets, suggesting that safe-haven or risk-off states are associated with a wider carry gap. IGOV is also positive, but its precision is market-dependent: it is significant in SPX and weaker in RUT. I therefore interpret IGOV as a slower foreign-bond and duration-related component, rather than as the most robust element of the 3ETF block.

The controls retain stable signs. The bid–ask measure is positive in all specifications, consistent with wider option-market trading frictions being associated with a larger carry-space wedge. NFCI is negative in all specifications. Because NFCI is estimated jointly with OIS terms and low-frequency asset components, I treat this sign as a conditional control relationship rather than as a standalone financial-conditions channel.

Table 6.7: Stability of LOYO training coefficients: 3ETF specification

Market	Specification	Variable	Mean coefficient	Min–Max	Sign frequency
SPX	3ETF	$GBM^{OIS,1Y}$	-0.133	[-0.254, -0.093]	+0/ – 10
SPX	3ETF	$GBM^{IEFA,70}$	-0.00840	[-0.01051, -0.00719]	+0/ – 10
SPX	3ETF	$GBM^{IGOV,441}$	0.03928	[0.01142, 0.05924]	+10/ – 0
SPX	3ETF	$GBM^{IAU,315}$	0.01527	[0.00831, 0.02916]	+10/ – 0
RUT	3ETF	$GBM^{OIS,1Y}$	-0.106	[-0.187, -0.066]	+0/ – 10
RUT	3ETF	$GBM^{IEFA,70}$	-0.00746	[-0.00950, -0.00624]	+0/ – 10
RUT	3ETF	$GBM^{IGOV,441}$	0.00924	[-0.02026, 0.03918]	+9/ – 1
RUT	3ETF	$GBM^{IAU,315}$	0.02316	[0.01610, 0.03564]	+10/ – 0

Table 6.7 shows that these signs are not driven by a single full-sample estimate. Across LOYO training folds, OIS 1Y and IEFA are negative in all 10 folds for both markets. IAU is positive in all 10 folds for both markets. IGOV is positive in all SPX folds and in 9 of 10 RUT folds. The coefficient structure used for out-of-sample evaluation is therefore broadly stable.

Overall, the coefficient evidence supports the same conclusion as the fit statistics. The carry gap is not fully summarized by the OIS-only path-risk block. The short OIS component remains important, but low-frequency outside-option components, especially developed ex-U.S. equity and gold, explain a stable residual part of the carry gap.

7 Drift versus Outside Options

This section connects the 3ETF result to the drift-extended specification of [Shin \(2026b\)](#). That paper shows that an own-index drift proxy, $\hat{\mu}$, improves the OIS-only carry-gap specification through an $OIS1Y \times \hat{\mu}^{504} \times \tau$ term. The question here is narrower: does this

drift proxy retain independent explanatory power once the broader outside-option block is included?

The exercise is an absorption test, not a rejection test of the drift channel. Because the true physical drift μ is unobserved, $\hat{\mu}^{504}$ is an empirical rolling-trend proxy. If it adds little after IEFA, IGOV, and IAU are included, the natural interpretation is not that drift is irrelevant. Rather, the own-index $\hat{\mu}$ proxy is likely a scalar projection of a broader physical-measure opportunity-cost state.

7.1 Incremental Fit

I compare the 3ETF specification with the 3ETF+drift specification. The 3ETF model includes OIS 1Y, IEFA, IGOV, IAU, BA^{med}/τ , and NFCI. The 3ETF+drift model adds $OIS1Y \times \hat{\mu}^{504} \times \tau$.

Table 7.1: Incremental performance of the drift proxy after the 3ETF block

Market	In sample			LOYO out of sample				
	R^2 3ETF	R^2 +drift	ΔR^2	Pooled R^2 3ETF	Pooled R^2 +drift	ΔR^2	Δ mean RMSE	
SPX	0.402	0.404	0.002	0.379	0.379	0.000	-0.02	
RUT	0.361	0.361	0.000	0.318	0.300	-0.018	0.15	

Table 7.1 shows limited incremental fit from adding the drift proxy after the 3ETF block. In sample, SPX gains only 0.002 in R^2 , while RUT is essentially unchanged. Out of sample, SPX pooled R^2 is unchanged at 0.379, whereas RUT pooled R^2 falls from 0.318 to 0.300. Mean RMSE improves only marginally in SPX and deteriorates in RUT.

Thus, the drift proxy does not provide a meaningful second layer of explanatory power once the outside-option block is already present. The evidence is consistent with the drift proxy containing useful low-frequency information in the OIS-only specification, but little independent information after the broader state vector is included.

7.2 Drift Loading

The coefficient evidence leads to the same conclusion. Table 7.2 reports the HAC drift loading in the full sample and the corresponding LOYO training-coefficient stability.

Table 7.2: Drift loading after the 3ETF block

Market	HAC coefficient	HAC s.e.	LOYO mean coefficient	LOYO sign frequency
SPX	0.027	0.019	0.025	+10/ - 0
RUT	-0.005	0.016	-0.010	+2/ - 8

Notes: The drift term is $OIS1Y \times \hat{\mu}^{504} \times \tau$. HAC standard errors use a 21-trading-day Newey–West lag. The LOYO sign frequency reports the sign of the training coefficient across the ten holdout folds.

The drift loading is statistically insignificant in both markets. In SPX, the coefficient is positive but small. It is also positive in all LOYO folds, so the direction does not disappear completely. However, the magnitude is too small to generate meaningful incremental fit after the 3ETF block is included. In RUT, the full-sample coefficient is slightly negative, and the LOYO coefficient is negative in 8 out of 10 folds. The drift proxy therefore does not behave as a stable additional state variable in RUT.

By contrast, the core 3ETF structure remains stable after the drift term is added. IEFA remains negative in both markets, IAU remains positive in both markets, and the OIS 1Y term remains negative. The stable structure is therefore not the additional own-index drift term, but the outside-option block layered on top of the short-horizon OIS component.

These results extend rather than overturn [Shin \(2026b\)](#). The earlier drift evidence shows that the carry gap is not fully explained by OIS-based path risk, trading frictions, and financial conditions. The present horse race shows that the own-index $\hat{\mu}$ proxy is not the final state variable. It is better interpreted as a scalar projection of a broader physical-measure investment-opportunity state. Once that state is represented by IEFA, IGOV, and IAU, little independent information remains in the own-index drift proxy.

8 Robustness

This section tests four threats to the main 3ETF result: broad-dollar exposure, common-factor collapse, lookback-horizon selection, and ETF-block choice. First, I remove a broad U.S.-dollar component from the IEFA, IGOV, and IAU price series and repeat the main analysis. Second, I use PCA and residualization to ask whether the 3ETF block collapses to a single latent factor. Third, I use a nested LOYO procedure to check whether horizon selection leaks information from the holdout year. Fourth, I compare the main developed ex-U.S. block with U.S.-centered and emerging-market-centered alternatives.

8.1 Dollar Adjustment

The first test asks whether the 3ETF result is merely a disguised broad-dollar cycle. I construct broad-dollar-adjusted ETF price series by subtracting the log broad-dollar index, DTWEXBGS, from the log prices of IEFA, IGOV, and IAU, and then recompute the rolling OLS slope series from these adjusted price paths. Appendix A describes the calendar alignment and previous-observation fill used to match DTWEXBGS to the ETF trading calendar.

This adjustment is deliberately mechanical. It is not intended to construct perfect currency-hedged ETF returns. It asks the narrower question of whether the 3ETF block continues to explain the carry gap after removing a broad U.S.-dollar component from the asset price series. As in the main 3ETF specification, the broad-dollar-adjusted model keeps $GBM^{OIS,1Y}$, drops $GBM^{OIS,10Y}$, and adds the adjusted IEFA, IGOV, and IAU GBM terms. The OIS-only baseline is unchanged.

Table 8.1: In-sample performance after broad-dollar adjustment

Metric	SPX	RUT
Baseline R^2	0.312	0.281
Main 3ETF R^2	0.402	0.361
FXN 3ETF R^2	0.403	0.368
FXN-main R^2	0.001	0.007
ΔR^2 vs. baseline	0.091	0.087
FXN RMSE (bp)	12.296	13.079

Table 8.1 shows that broad-dollar adjustment does not weaken the in-sample result. In SPX, R^2 changes from 0.402 in the main 3ETF specification to 0.403 after dollar adjustment. In RUT, it rises from 0.361 to 0.368. The adjusted 3ETF block therefore preserves essentially the same fit gain over the OIS-only baseline.

If the main result were only a broad-dollar factor in disguise, removing the broad-dollar component from the ETF price paths should materially reduce explanatory power. It does not. Broad-dollar variation may still be part of the global state, especially for the unhedged foreign-bond component, but it does not account for the aggregate explanatory content of the 3ETF block.

8.1.1 Out-of-Sample Performance

Table 8.2: LOYO out-of-sample performance: baseline, main 3ETF, and broad-dollar-adjusted 3ETF

Market	Specification	Mean R^2	Median R^2	Pooled R^2	Mean RMSE (bp)	Mean correlation
SPX	Baseline	0.059	0.130	0.221	13.947	0.205
SPX	Main 3ETF	0.288	0.195	0.379	12.369	0.373
SPX	FXN 3ETF	0.283	0.212	0.373	12.461	0.399
RUT	Baseline	0.075	0.108	0.171	15.075	0.243
RUT	Main 3ETF	0.237	0.211	0.318	13.825	0.356
RUT	FXN 3ETF	0.251	0.222	0.320	13.786	0.369

Table 8.2 shows that the broad-dollar-adjusted 3ETF block also survives LOYO validation. In SPX, pooled OOS R^2 changes only from 0.379 in the main 3ETF model to 0.373 after dollar adjustment. In RUT, it changes from 0.318 to 0.320. Mean R^2 , median R^2 , RMSE, and correlation are also close to the main 3ETF results.

Thus, the OOS result is not simply a comparison against the OIS-only baseline. The dollar-adjusted 3ETF block performs almost as well as the original 3ETF block. This is the key evidence against the interpretation that the main result is just an unremoved broad-dollar cycle.

Table 8.3: Year-by-year LOYO out-of-sample performance: SPX, broad-dollar-adjusted 3ETF

Holdout year	Baseline			FXN 3ETF		
	R^2	RMSE (bp)	Corr.	R^2	RMSE (bp)	Corr.
2016	0.185	8.970	0.194	-0.015	10.012	0.389
2017	0.074	10.069	0.226	0.274	8.918	0.409
2018	0.221	26.304	0.259	0.167	27.200	0.205
2019	0.023	8.934	-0.011	0.202	8.074	0.404
2020	-1.221	18.423	-0.294	0.061	11.980	0.409
2021	0.416	7.600	0.064	0.556	6.629	0.123
2022	0.357	16.040	0.347	0.491	14.275	0.300
2023	0.571	15.725	0.438	0.695	13.267	0.513
2024	-0.016	15.428	0.589	0.221	13.506	0.748
2025	-0.022	11.980	0.242	0.178	10.744	0.487
Mean	0.059	13.947	0.205	0.283	12.461	0.399
Median	0.130			0.212		
Pooled	0.221			0.373		

Table 8.4: Year-by-year LOYO out-of-sample performance: RUT, broad-dollar-adjusted 3ETF

Holdout year	Baseline			FXN 3ETF		
	R^2	RMSE (bp)	Corr.	R^2	RMSE (bp)	Corr.
2016	-0.350	12.787	0.069	0.183	9.952	0.300
2017	-0.152	10.498	0.142	0.038	9.592	0.353
2018	0.213	18.830	0.121	0.133	19.763	0.235
2019	-0.041	11.088	-0.007	0.066	10.504	0.459
2020	-0.587	22.437	0.102	0.281	15.100	0.422
2021	0.477	12.368	0.431	0.502	12.071	0.382
2022	0.308	16.619	0.368	0.265	17.130	0.221
2023	0.661	13.922	0.354	0.738	12.247	0.454
2024	0.153	14.005	0.598	0.260	13.086	0.494
2025	0.064	18.193	0.248	0.041	18.411	0.368
Mean	0.075	15.075	0.243	0.251	13.786	0.369
Median	0.108			0.222		
Pooled	0.171			0.320		

Tables 8.3 and 8.4 report the year-by-year results. The broad-dollar-adjusted 3ETF specification beats the baseline in 8 of 10 SPX holdouts and 7 of 10 RUT holdouts. It also

produces positive OOS R^2 in 9 of 10 SPX holdouts and in all 10 RUT holdouts, compared with 7 and 6 positive holdouts for the baseline.

The 2020 holdout shows that the stress-year repair is not eliminated by dollar adjustment. In SPX, the baseline OOS R^2 is -1.221 , while the adjusted 3ETF model gives 0.061 . In RUT, the corresponding values are -0.587 and 0.281 . The adjusted asset block therefore still mitigates the largest level-calibration failure of the OIS-only baseline.

The result is not uniform across every year. The adjusted specification is weaker than the baseline in SPX in 2016 and 2018, and in RUT in 2018, 2022, and 2025. I therefore interpret the test as evidence of out-of-sample stability after dollar adjustment, not as a claim of uniformly superior forecasting performance in every holdout year.

8.1.2 Coefficient Structure

The coefficient evidence clarifies which parts of the 3ETF block survive dollar adjustment. Rather than re-estimating the full economic interpretation of all controls, I focus on the adjusted asset terms and the retained OIS 1Y component.

Table 8.5: Key coefficients after broad-dollar adjustment

Variable	SPX coefficient	SPX LOYO signs	RUT coefficient	RUT LOYO signs
$GBM^{OIS,1Y}$	-0.1735^{***} (0.0450)	+0/ - 10	-0.1157^{***} (0.0275)	+0/ - 10
$GBM^{IEFA,FXN,70}$	-0.00749^{***} (0.00122)	+0/ - 10	-0.00620^{***} (0.00097)	+0/ - 10
$GBM^{IGOV,FXN,441}$	0.01264 (0.01259)	+9/ - 1	0.00252 (0.00983)	+8/ - 2
$GBM^{IAU,FXN,315}$	0.02245^{***} (0.00603)	+10/ - 0	0.02425^{***} (0.00415)	+10/ - 0

Notes: Parentheses report date-based HAC Newey–West standard errors with a 21-trading-day lag. ***, **, and * denote significance at the 1%, 5%, and 10% levels. LOYO signs report the sign frequency of the corresponding training coefficient across the ten holdout folds.

Table 8.5 shows that the dollar-adjusted signal is concentrated in IEFA and IAU. The adjusted IEFA term is negative, highly significant, and negative in every LOYO fold for both markets. The adjusted IAU term is positive, highly significant, and positive in every LOYO fold. These two components therefore carry the most stable FX-orthogonal part of the 3ETF block.

IGOV behaves differently. After broad-dollar adjustment, its coefficient remains positive

but is no longer statistically significant in either market, and its LOYO sign stability weakens, especially in RUT. This suggests that the original IGOV signal is partly dollar-sensitive. IGOV is still useful as a slow foreign-bond state variable in the main specification, but it is not the clean FX-orthogonal core of the result.

The OIS 1Y term remains negative and significant in both markets, with stable LOYO signs. Dollar adjustment therefore does not eliminate the short-horizon OIS path-risk channel. Overall, the test supports the main interpretation: the 3ETF result is not reducible to a broad-dollar cycle, but its components are heterogeneous. IEFA and IAU provide robust dollar-adjusted channels, while IGOV is a weaker dollar-sensitive slow component.

8.2 Common-Factor Tests

This subsection asks whether the 3ETF block is only repeated exposure to one latent global factor. If IEFA, IGOV, and IAU were close substitutes for the same cycle, the asset-slope series should be highly correlated and the first principal component should dominate their variation.

The pairwise correlations are modest: 0.088 between IEFA and IGOV, 0.170 between IEFA and IAU, and 0.381 between IGOV and IAU. Thus, even before rotation, the three slope series do not look like different labels for a single common factor.

Table 8.6: Principal-component decomposition of the three asset-slope series

Component	Explained variance	IEFA loading	IGOV loading	IAU loading
PC1	48.5%	0.375	0.637	0.674
PC2	31.2%	0.913	-0.382	-0.146
PC3	20.3%	-0.164	-0.670	0.724

Table 8.6 confirms that the 3ETF block is not one-dimensional. PC1 explains only 48.5% of total variance and loads mainly on IGOV and IAU. PC2 explains another 31.2% and is strongly IEFA-dominant. The foreign-equity component therefore does not collapse into the slower IGOV–IAU component. PC3 mainly separates IGOV from IAU.

I also replace the raw asset GBM terms with three orthogonal principal-component GBM terms. Because the three PCs preserve the linear span of the original asset block, the in-sample fit is unchanged: $R^2 = 0.402$ in SPX and $R^2 = 0.361$ in RUT, the same as in the raw 3ETF specification. The point is not that PCA raises fit, but that the fit is not an artifact of collinearity among the raw ETF variables. The explanatory power belongs to the low-frequency state space spanned by the assets.

Finally, I residualize each asset slope on the other two. The first-stage R^2 values are 0.029 for IEFA, 0.146 for IGOV, and 0.164 for IAU. IEFA is therefore almost orthogonal to the other two slopes, and even IGOV and IAU retain substantial asset-specific variation. The residualized components continue to explain the carry gap, indicating that asset-specific variation outside the other two slopes still contains alignment information.

Overall, these tests weaken the single-common-factor interpretation. The 3ETF block contains a slow IGOV–IAU component, a distinct IEFA-dominant component, and residual variation separating IGOV from IAU. It is better interpreted as a multi-channel outside-option structure with heterogeneous frequencies, not as three noisy versions of one latent global factor.

8.3 Nested Horizon Selection

The main specification fixes the asset lookback horizons at 70 trading days for IEFA, 441 days for IGOV, and 315 days for IAU. Because these horizons are selected from asset-by-asset horizon profiles, full-sample horizon choice could overstate out-of-sample performance. I address this concern with a nested LOYO procedure.

For each holdout year, I first remove that year from the sample. I then select the IEFA, IGOV, and IAU lookback windows using only the remaining training years, with the equal-weighted average of SPX and RUT in-sample R^2 as the objective. The selected horizons are then fixed, coefficients are estimated on the same training years, and performance is evaluated in the excluded holdout year. Thus, the holdout year is used neither for coefficient estimation nor for horizon selection.

Table 8.7: Nested horizon selection: distribution of selected lookback windows

Asset	Mean	Median	Mode	Min	Max	Unique values
IEFA	78.1	79.0	79	65	87	5
IGOV	317.8	319.0	318	264	366	7
IAU	325.6	328.5	322	309	335	8

Table 8.7 shows that the nested search does not mechanically reproduce the main horizons. The selected IGOV horizon is shorter than the 441-day main specification horizon. However, the qualitative frequency ordering remains intact: IEFA is repeatedly selected at a short horizon, while IGOV and IAU are selected at slower horizons. Applying the same search to the full sample selects IEFA = 79, IGOV = 319, and IAU = 324. No fold-level solution lies on the search boundary.

Table 8.8: Nested horizon-selection LOYO performance

Market/score	Statistic	Baseline	3ETF	Difference/count
SPX	Mean R^2	0.059	0.281	0.222
	Median R^2	0.130	0.197	0.067
	Positive ΔR^2 years	–	–	8/10
RUT	Mean R^2	0.075	0.212	0.137
	Median R^2	0.108	0.134	0.026
	Positive ΔR^2 years	–	–	6/10
Equal-weight	Mean R^2	0.067	0.246	0.180
	Median R^2	0.045	0.163	0.118
	Positive ΔR^2 years	–	–	8/10

Table 8.8 shows that the asset-return extension continues to improve LOYO performance even when horizons are selected only inside the training sample. Mean OOS R^2 rises from 0.059 to 0.281 in SPX and from 0.075 to 0.212 in RUT. The equal-weighted score rises from 0.067 to 0.246. The gain is positive in 8 out of 10 SPX holdouts, 6 out of 10 RUT holdouts, and 8 out of 10 equal-weighted holdouts.

The gains are smaller than in the fixed-horizon main specification, which is expected because the nested design removes full-sample horizon information. But the improvement over the OIS-only baseline remains. Using yearly RMSE and holdout sample size to compute pooled OOS R^2 , the nested score rises from 0.221 to 0.336 in SPX and from 0.171 to 0.287 in RUT. In the 2020 stress holdout, the nested 3ETF specification also repairs much of the baseline failure: OOS R^2 improves from -1.221 to 0.054 in SPX and from -0.587 to 0.256 in RUT.

Overall, the nested exercise supports the main conclusion. Even when lookback windows are selected using training-sample information only, the data again select a fast foreign-equity component and slower foreign-bond and gold components, and the 3ETF block retains higher out-of-sample explanatory power than the OIS-only baseline. The main result is therefore difficult to explain as an artifact of ex post full-sample horizon selection alone.

8.4 Alternative Blocks

Finally, I test whether the main result depends on the specific IEFA–IGOV–IAU combination. I compare the main developed ex-U.S. block with two alternatives: a U.S.-centered block, VTI(42), BND(252), and IAU(300), and an emerging-market-centered block, IEMG(63), EBND(126), and IAU(300). The lookback windows for the alternative blocks

are selected through separate horizon scans. As in the main 3ETF specification, each asset-augmented model keeps $GBM^{OIS,1Y}$ and excludes $GBM^{OIS,10Y}$.

Table 8.9: Performance comparison across alternative 3ETF asset blocks

Specification	Market	IS R^2	Mean OOS R^2	Pooled OOS R^2
Baseline	SPX	0.312	0.059	0.221
	RUT	0.281	0.075	0.171
Main 3ETF	SPX	0.402	0.288	0.379
	RUT	0.361	0.237	0.318
U.S.-centered	SPX	0.364	0.253	0.326
	RUT	0.339	0.209	0.270
Emerging-market	SPX	0.385	0.243	0.331
	RUT	0.362	0.262	0.342

Notes: Main 3ETF = IEFA(70) + IGOV(441) + IAU(315); U.S.-centered = VTI(42) + BND(252) + IAU(300); Emerging-market = IEMG(63) + EBND(126) + IAU(300). Out-of-sample performance is evaluated using LOYO validation. All asset-augmented specifications keep $GBM^{OIS,1Y}$ and exclude $GBM^{OIS,10Y}$.

Table 8.9 shows that the asset-extension result does not depend on a single ETF combination. All three asset-augmented blocks improve on the OIS-only baseline in both markets, both in sample and out of sample. The main developed ex-U.S. block gives the strongest SPX performance, with pooled OOS $R^2 = 0.379$. In RUT, the emerging-market block performs best out of sample, with pooled OOS $R^2 = 0.342$.

The weaker performance of the U.S.-centered block should be interpreted conditionally. The baseline already contains substantial U.S.-centered information through OIS rates, VIX/RVX, bid-ask frictions, and NFCI. The foreign-tilted blocks therefore appear to contain more residual outside-option information after the baseline controls are included.

Overall, the alternative-block evidence supports the main interpretation. The IEFA-IGOV-IAU block is the most balanced specification, especially for SPX, but it is not a uniquely lucky ETF combination. Other asset-allocation blocks also improve on the baseline, which suggests that the carry gap is aligned with residual outside-option states more generally.

9 Discussion

9.1 A Conditional Outside-Option Interpretation

The 3ETF result should be interpreted conditionally, not as a claim that foreign assets are unconditionally better outside-option proxies than U.S. assets. The baseline is already strongly U.S.-centered. OIS rates capture the funding component, VIX and RVX enter the GBM scale as high-frequency market-specific volatility states, BA^{med}/τ captures option-market trading frictions, and NFCI partly absorbs slow U.S. financial-condition and risk-bearing variation. The asset-extension exercise therefore asks which asset-return components contain incremental information after this baseline state vector has already been controlled for.

Equivalently, the relevant object is not the unconditional information in an asset-return component Z_a , but its residual information after conditioning on the baseline:

$$\Delta R_a^2 = R^2(CG | X_{\text{base}}, Z_a) - R^2(CG | X_{\text{base}}).$$

The empirical result is therefore not that U.S. assets are irrelevant. Rather, much of the U.S.-centered state space is already represented by the baseline controls, leaving less residual room for U.S. asset returns to improve the regression.

This interpretation helps explain why the developed ex-U.S. block performs better than the U.S.-centered block. VTI and BND may be valid outside options in economic terms, but their incremental contribution is evaluated after OIS rates, VIX/RVX, NFCI, and option-market frictions have already been partialled out. IEFA, IGOV, and IAU appear to contain residual global information less directly spanned by this U.S.-centered baseline.

The components of the 3ETF block should therefore be read as conditional residual channels rather than structural pricing factors. IEFA captures a global risk-bearing component not fully summarized by domestic volatility and financial conditions. IAU captures a safe-haven or liquidity-demand component. IGOV is a more conditional slow component, combining foreign duration, safe-asset demand, and dollar-sensitive global funding variation. The point is not that these assets directly price U.S. index options, but that they proxy for residual outside-option states faced by finite-capital parity enforcers.

This interpretation is related in spirit to the ICAPM logic of [Merton \(1973\)](#). Finite-capital arbitrageurs care not only about the current funding rate, but also about the investment-opportunity set available while the parity trade is being financed and margined. The exercise here is more modest than an ICAPM estimation: I do not recover a structural stochastic discount factor or identify primitive state variables. The ETF terms are reduced-form proxies

for residual investment-opportunity states after conditioning on the U.S.-centered baseline.

9.2 Drift, NFCI, Dollar Exposure, and Common Factors

The drift evidence supports the same partial-out interpretation. In Shin (2026b), adding the own-index drift proxy $\hat{\mu}^{504}$ to the OIS-only baseline reduces the absolute NFCI loading in both markets. In SPX, the NFCI coefficient moves from -25.839 to -19.577 . In RUT, it moves from -23.961 to -22.286 . By contrast, the BA^{med}/τ coefficient is largely unchanged. This pattern suggests that the drift proxy absorbs part of the slow U.S. financial-condition state rather than the option-market trading-friction channel.

The 3ETF horse race extends this logic. The own-index drift proxy improves the OIS-only specification, but it has little independent explanatory power after IEFA, IGOV, and IAU are included. This does not reject the drift channel. It suggests that $\hat{\mu}^{504}$ is a scalar projection of a broader physical-measure investment-opportunity state. The 3ETF block captures that state more flexibly, leaving less residual role for the single own-index drift term.

The broad-dollar adjustment and common-factor tests further discipline this interpretation. If the 3ETF result were merely a disguised broad-dollar cycle, removing a broad U.S.-dollar component from the ETF price paths should have produced a large deterioration. It does not. The adjusted 3ETF block performs close to the original 3ETF specification. At the coefficient level, however, IGOV weakens after dollar adjustment, indicating that its original signal is partly dollar-sensitive.

The PCA and residualization tests also reject the view that the 3ETF block is only repeated exposure to one latent factor. The first principal component does not dominate the three asset-slope series, the IEFA-dominant component remains distinct, and residualized asset components continue to explain the carry gap. The evidence is therefore better read as a small multi-channel outside-option state space, not as one hidden global factor.

9.3 P–Q Alignment and Limits

The results should be interpreted as reduced-form P–Q alignment, not as structural P-to-Q recovery. Put–call parity remains a terminal-payoff identity. The physical-measure asset components do not enter the payoff identity, and the results do not imply a failure of risk-neutral pricing.

The mechanism is implementation-based. The carry gap is a Q -measure carry-space object extracted from option-implied discounting. But enforcing put–call parity requires capital, margin support, funding capacity, and balance-sheet usage before maturity. The

arbitrageur who supplies this enforcement capital faces physical-measure outside options. Thus, even though terminal parity is risk-neutral, the implementation premium embedded in the carry gap can be aligned with physical-measure investment-opportunity states.

Several limitations remain. The regressions are reduced-form and should not be interpreted as causal estimates, a complete stochastic discount factor, or a structural model of intermediary optimization. The selected ETFs are proxies, not primitive state variables. The lookback horizons and alternative-block tests discipline the specification, but they do not identify a unique structural state vector.

The main takeaway is conditional. The carry gap is not fully explained by OIS-only funding variables, and it is not fully summarized by the own-index drift proxy. After U.S.-centered funding, volatility, trading-friction, and financial-condition controls are included, the remaining outside-option information is more visible in global and ex-U.S. asset components. The 3ETF specification is therefore best understood as a parsimonious proxy for residual outside-option costs of finite arbitrage capital, rather than as a structural claim that foreign assets price U.S. options.

10 Conclusion

This paper tests whether the carry gap in put–call parity is fully explained by OIS-based discounting, volatility, trading-friction, and financial-condition variables, or whether it also contains residual information aligned with outside investment opportunities faced by finite arbitrage capital. The evidence supports the latter view. Adding the 3ETF block of IEFA, IGOV, and IAU improves the OIS-based baseline in both SPX and RUT options, and the improvement survives leave-one-year-out validation and a range of robustness checks, including broad-dollar adjustment, common-factor tests, nested horizon selection, and alternative asset-block specifications.

The economic interpretation is conditional. The result should not be read as a claim that foreign assets are unconditionally better outside-option proxies than U.S. assets. The baseline already contains substantial U.S.-centered information through OIS rates, VIX/RVX, bid–ask frictions, and NFCI. The 3ETF block is therefore informative because it captures residual global investment-opportunity states after domestic funding, volatility, trading-friction, and financial-condition variables have already been controlled for. In this sense, IEFA, IGOV, and IAU are not structural pricing factors, but reduced-form proxies for marginal outside-option information left outside the baseline state vector.

The drift evidence is complementary to this interpretation. The own-index drift proxy $\hat{\mu}$ improves the OIS-only baseline, but contributes little after the 3ETF block is included. This

pattern suggests that $\hat{\mu}$ is not a competing explanation, but a scalar projection of a broader physical-measure investment-opportunity state. The 3ETF block provides a more flexible representation of that state, while the robustness tests show that its explanatory power is not reducible to a broad-dollar factor or to a single latent common component.

The results should be interpreted as reduced-form P - Q alignment, not as structural P -to- Q recovery. Put-call parity remains a terminal no-arbitrage identity, and the physical-measure asset components do not enter option payoffs directly. The point is that enforcing the parity relation in actual markets is path-dependent and capital-using. Before maturity, arbitrageurs face variation margin, funding needs, interim losses, liquidation risk, and alternative uses of capital. The central contribution is therefore to show that a nearly closed no-arbitrage relation can still leave a carry-space trace of the opportunity cost of finite arbitrage capital. The carry gap is a risk-neutral parity object in construction, but its enforcement can reflect physical-measure investment opportunities.

Funding

This research did not receive any specific grant from funding agencies in the public, commercial, or not-for-profit sectors.

Declaration of AI usage in manuscript preparation

During the preparation of this manuscript, the author used ChatGPT (OpenAI) and Claude (Anthropic) for language refinement and structural clarity. All outputs were reviewed and edited by the author, who takes full responsibility for the content.

Declaration of interest

The author declares no competing interests.

References

- Stoll, H. R. (1969). The Relationship between Put and Call Option Prices. *The Journal of Finance*, 24(5), 801–824. <https://doi.org/10.1111/j.1540-6261.1969.tb01694.x>
- Merton, R. C. (1973). An Intertemporal Capital Asset Pricing Model. *Econometrica*, 41(5), 867–887. <https://doi.org/10.2307/1913811>
- Gould, J. P., & Galai, D. (1974). Transaction Costs and the Relationship between Put and Call Prices. *Journal of Financial Economics*, 1(2), 105–129. [https://doi.org/10.1016/0304-405X\(74\)90001-4](https://doi.org/10.1016/0304-405X(74)90001-4)
- Ross, S. A. (1976). The arbitrage theory of capital asset pricing. *Journal of Economic Theory*, 13(3), 341–360. [https://doi.org/10.1016/0022-0531\(76\)90046-6](https://doi.org/10.1016/0022-0531(76)90046-6)
- Klemkosky, R. C., & Resnick, B. G. (1979). Put–Call Parity and Market Efficiency. *The Journal of Finance*, 34(5), 1141–1155. <https://doi.org/10.1111/j.1540-6261.1979.tb00061.x>
- Chen, N. F., Roll, R., & Ross, S. A. (1986). Economic Forces and the Stock Market. *Journal of Business*, 59, 383–403. <https://doi.org/10.1086/296344>
- Campbell, J. Y. (1993). Intertemporal asset pricing without consumption data. *The American Economic Review*, 83(3), 487–512. <http://www.jstor.org/stable/2117530>
- Fama, E. F., & French, K. R. (1993). Common risk factors in the returns on stocks and bonds. *Journal of Financial Economics*, 33(1), 3–56. [https://doi.org/10.1016/0304-405X\(93\)90023-5](https://doi.org/10.1016/0304-405X(93)90023-5)
- Shleifer, A., & Vishny, R. W. (1997). The Limits of Arbitrage. *The Journal of Finance*, 52(1), 35–55. <https://doi.org/10.1111/j.1540-6261.1997.tb03807.x>
- Ackert, L. F., & Tian, Y. S. (2001). Efficiency in Index Options Markets and Trading in Stock Baskets. *Journal of Banking & Finance*, 25(9), 1607–1634. [https://doi.org/10.1016/S0378-4266\(00\)00145-X](https://doi.org/10.1016/S0378-4266(00)00145-X)
- Gromb, D., & Vayanos, D. (2002). Equilibrium and Welfare in Markets with Financially Constrained Arbitrageurs. *Journal of Financial Economics*, 66(2–3), 361–407. [https://doi.org/10.1016/S0304-405X\(02\)00228-3](https://doi.org/10.1016/S0304-405X(02)00228-3)
- Campbell, J. Y., & Vuolteenaho, T. (2004). Bad beta, good beta. *American Economic Review*, 94(5), 1249–1275. <https://doi.org/10.1257/0002828043052240>

- Ofek, E., Richardson, M., & Whitelaw, R. F. (2004). Limited arbitrage and short sales restrictions: evidence from the options markets. *Journal of Financial Economics*, 74(2), 305–342. <https://doi.org/10.1016/j.jfineco.2003.05.008>
- Petkova, R. (2006). Do the Fama–French factors proxy for innovations in predictive variables? *The Journal of Finance*, 61(2), 581–612. <https://doi.org/10.1111/j.1540-6261.2006.00849.x>
- Bollerslev, T., Tauchen, G., & Zhou, H. (2009). Expected Stock Returns and Variance Risk Premia. *The Review of Financial Studies*, 22(11), 4463–4492. <https://doi.org/10.1093/rfs/hhp008>
- Brunnermeier, M. K., & Pedersen, L. H. (2009). Market Liquidity and Funding Liquidity. *The Review of Financial Studies*, 22(6), 2201–2238. <https://doi.org/10.1093/rfs/hhn098>
- Gârleanu, N., & Pedersen, L. H. (2011). Margin-based asset pricing and deviations from the law of one price. *The Review of Financial Studies*, 24(6), 1980–2022. <https://doi.org/10.1093/rfs/hhr027>
- Mitchell, M., & Pulvino, T. (2012). Arbitrage Crashes and the Speed of Capital. *Journal of Financial Economics*, 104(3), 469–490. <https://doi.org/10.1016/j.jfineco.2011.09.002>
- He, Z., & Krishnamurthy, A. (2013). Intermediary asset pricing. *American Economic Review*, 103(2), 732–770. <https://doi.org/10.1257/aer.103.2.732>
- Adrian, T., Etula, E., & Muir, T. (2014). Financial intermediaries and the cross-section of asset returns. *The Journal of Finance*, 69(6), 2557–2596. <https://doi.org/10.1111/jofi.12189>
- Ross, S. (2015). The Recovery Theorem. *The Journal of Finance*, 70(2), 615–648. <https://doi.org/10.1111/jofi.12092>
- He, Z., Kelly, B., & Manela, A. (2017). Intermediary asset pricing: New evidence from many asset classes. *Journal of Financial Economics*, 126(1), 1–35. <https://doi.org/10.1016/j.jfineco.2017.08.002>
- Martin, I. (2017). What Is the Expected Return on the Market? *The Quarterly Journal of Economics*, 132(1), 367–433. <https://doi.org/10.1093/qje/qjw034>
- Du, W., Tepper, A., & Verdelhan, A. (2018). Deviations from Covered Interest Rate Parity. *The Journal of Finance*, 73(3), 915–957. <https://doi.org/10.1111/jofi.12620>

- Azzone, M., & Baviera, R. (2021). Synthetic Forwards and Cost of Funding in the Equity Derivative Market. *Finance Research Letters*, 41, 101841. <https://doi.org/10.1016/j.frl.2020.101841>
- Muravyev, D., Pearson, N. D., & Pollet, J. M. (2025). Why does options market information predict stock returns? *Journal of Financial Economics*, 172, 104153. <https://doi.org/10.1016/j.jfineco.2025.104153>
- Shin, U. (2026). The Cost of a Free Lunch. *SSRN Working Paper*, No. 6407379 <https://dx.doi.org/10.2139/ssrn.6407379>
- Shin, U. (2026). The P behind Q. *SSRN Working Paper*, No. 6762800 <https://dx.doi.org/10.2139/ssrn.6762800>
- Chicago Fed National Financial Conditions Index [NFCI] (2026a), retrieved from FRED, Federal Reserve Bank of St. Louis, April 3, 2026. <https://fred.stlouisfed.org/series/NFCI>
- Board of Governors of the Federal Reserve System (US) (2026b). Nominal Broad U.S. Dollar Index [DTWEXBGS], retrieved from FRED, Federal Reserve Bank of St. Louis, April 3, 2026. <https://fred.stlouisfed.org/series/DTWEXBGS>.
- ThetaData (2026). Historical SPX and RUT option NBBO data. Retrieved April 3, 2026, from <https://www.thetadata.net>.

A Data and Methodological Details

This appendix summarizes the implementation details behind the carry-gap construction, asset-return variables, drift proxy, and in-sample and out-of-sample evaluation. The main text focuses on economic interpretation and model comparison; this appendix records the data processing and estimation steps needed for replication.

A.1 Data and Analysis Sample

The option data are minute-level NBBO quotes from ThetaData. The analysis uses the period from January 4, 2016 to October 31, 2025, which is the common sample over which option-market information and the OIS discount curve are both available. All main results are computed on this common sample.

SPX and RUT options are European-style index options. I therefore do not adjust the put–call-parity construction for early-exercise premia. The empirical pipeline is implemented in MATLAB R2025b.

A.2 Option-Implied Discount Factors and Carry-Gap Construction

I identify option-implied discount factors using the synthetic-forward procedure of [Azzone and Baviera \(2021\)](#). For a European call and put with the same date t , maturity T , and strike K , put–call parity can be written as

$$C_t(K, T) - P_t(K, T) = B_t(T)(F_t(T) - K), \quad (6)$$

where $B_t(T)$ is the market-implied discount factor and $F_t(T)$ is the forward value for maturity T . Define the synthetic forward as

$$G_t(K, T) = C_t(K, T) - P_t(K, T). \quad (7)$$

Then

$$F_t(T) = \frac{G_t(K, T)}{B_t(T)} + K. \quad (8)$$

Within each date–maturity cell, $B_t(T)$ is identified as the value that makes the recovered forward price flat across strikes. Operationally, I use the cross-sectional linear relation between synthetic forwards and strikes to estimate $\hat{B}_t(T)$ and $\hat{F}_t(T)$ jointly.

The benchmark discount factor is constructed from the OIS curve. I bootstrap daily

OIS data to recover maturity-specific discount factors and zero rates, and then interpolate maturity-matched OIS discount factors to option maturities. As in equation (1) in the main text, the carry gap is the annualized wedge between the option-implied discount factor and the OIS discount factor. The empirical analysis uses $CG_{i,t}^{bp}$, measured in basis points.

A.3 Sample Filters and Date–Maturity Aggregation

The preprocessing is designed to make the cross-sectional identification of $\hat{B}_t(T)$ stable. I first keep only call–put pairs with the same strike and maturity. I then apply rule-based filters that remove quotes with abnormal prices, excessive bid–ask spreads, insufficient strike coverage within a date–maturity cell, or unstable OIS curve construction. The same filters are applied symmetrically to SPX and RUT and are fixed before any regression estimation.

For each market, I construct date–maturity cells and estimate the option-implied discount factor within each eligible cell. I then form a date–maturity panel of carry gaps. When multiple eligible observations remain within the same date–maturity cell, I aggregate them using the median. Median aggregation reduces sensitivity to transient quote noise, stale quotes, and isolated cross-sectional outliers.

A.4 Asset-Return-Based Low-Frequency Components

The asset-return extension constructs low-frequency return components from ETF prices representing broad asset classes. The candidate ETFs are VTI, IEFA, IEMG, BND, SCHP, IGOV, EBND, IAU, VNQ, and VNQI. They represent U.S. equity, developed ex-U.S. equity, emerging-market equity, U.S. aggregate bonds, U.S. inflation-linked bonds, international sovereign bonds, emerging-market sovereign bonds, gold, U.S. REITs, and ex-U.S. REITs. The main 3ETF specification uses IEFA, IGOV, and IAU.

For asset a , the n -day low-frequency component is the OLS slope of the log price path over the past n trading days:

$$\log P_{a,t-n+\ell} = \alpha_{a,t}^{(n)} + b_{a,t}^{(n)}\ell + u_{a,t-n+\ell}, \quad \ell = 0, 1, \dots, n-1. \quad (9)$$

The slope uses information available through $t-1$; the contemporaneous price at date t is not used. This timing convention prevents the asset-return component from using information from the same date as the carry-gap observation.

The OLS slope is less sensitive to endpoint noise than a simple cumulative return. In the asset-based GBM term, $b_{a,t}^{(n)}$ enters as the rate-like opportunity-cost component. Because OIS rates are observed in percentage points, the OIS-based GBM term uses $OIS/100$. By

contrast, $b_{a,t}^{(n)}$ is a log-price slope, so no additional 1/100 adjustment is applied.

A.5 Own-Index Drift Proxy

The drift specification constructs a rolling drift proxy from the own-index total-return path. Let $TR_{i,t}$ denote the total-return index for market $i \in \{\text{SPX}, \text{RUT}\}$. The n -day drift proxy is the slope from

$$\log TR_{i,t-n+\ell} = a_{i,t}^{(n)} + b_{i,t}^{(n)}\ell + u_{i,t-n+\ell}^{(n)}, \quad \ell = 0, 1, \dots, n-1. \quad (10)$$

The drift comparison in the main text uses $n = 504$ trading days. The daily slope is annualized as

$$\hat{\mu}_{i,t}^{ann} = 252b_{i,t}^{(n)}. \quad (11)$$

Here $\hat{\mu}_{i,t}^{ann}$ is not an observed expected return. It is a reduced-form empirical drift proxy extrapolated from the past total-return path.

The drift-preserving GBM proxy is

$$GBM_{i,t}^{\hat{\mu}, \text{OIS}, 1Y} = 10^4 \cdot \frac{OIS1Y_t}{100} \cdot \hat{\mu}_{i,t}^{ann} \cdot \tau_{i,t}. \quad (12)$$

This term does not assume that $\hat{\mu}$ is the true physical drift μ . It is an empirical $r\hat{\mu}\tau$ proxy for the theoretical $r\mu\tau$ structure that appears in the support-capital approximation when physical drift is preserved.

A.6 Broad-Dollar Adjustment

The broad-dollar robustness test examines whether the foreign-asset components simply proxy for a common U.S.-dollar cycle. I use the broad-dollar index DTWEXBGS to construct mechanically adjusted price paths for IEFA, IGOV, and IAU. Specifically, I subtract the log broad-dollar index from each ETF log price and then recompute the rolling OLS slopes using the same procedure as in equation (9).

This adjustment should not be interpreted as constructing fully currency-hedged ETF returns. It is a diagnostic that removes a broad U.S.-dollar component from the ETF price paths. The DTWEXBGS calendar does not perfectly match the ETF trading calendar, so missing values are forward-filled using the most recent available observation before the adjusted slopes are computed.

The broad-dollar-adjusted specification follows the main 3ETF specification. It keeps $GBM^{\text{OIS}, 1Y}$, excludes $GBM^{\text{OIS}, 10Y}$, and includes GBM terms based on adjusted IEFA, IGOV,

and IAU slopes. The OIS-only baseline is unchanged and includes both OIS 1Y and OIS 10Y GBM terms.

A.7 Comparison Specifications

The main analysis compares four specifications:

$$\begin{array}{ll}
 \text{Baseline:} & GBM^{\text{OIS},1Y}, GBM^{\text{OIS},10Y}, BA^{\text{med}}/\tau, NFCI, \\
 \text{Drift:} & \text{Baseline} + GBM^{\hat{\mu},\text{OIS},1Y}, \\
 \text{3ETF:} & GBM^{\text{OIS},1Y}, GBM^{\text{IEFA},70}, GBM^{\text{IGOV},441}, GBM^{\text{IAU},315}, BA^{\text{med}}/\tau, NFCI, \\
 \text{3ETF+drift:} & \text{3ETF} + GBM^{\hat{\mu},\text{OIS},1Y}.
 \end{array}$$

The 3ETF specification excludes $GBM^{\text{OIS},10Y}$ because the long-horizon OIS component strongly overlaps with the low-frequency outside-option component associated with IGOV. Including both terms destabilizes coefficient interpretation, while dropping OIS 10Y causes only limited loss in explanatory power. The preferred specification therefore keeps OIS 1Y as the short-horizon risk-free opportunity-cost channel and replaces the long-horizon component with the 3ETF outside-option block.

A.8 Regression Estimation and Out-of-Sample Evaluation

All main regressions are estimated separately for SPX and RUT. Coefficient inference uses date-based HAC Newey–West standard errors with a fixed 21-trading-day lag. This lag allows for approximately one month of residual autocorrelation and is longer than the standard automatic lag rule for the daily sample, which selects about 8 trading days.

Out-of-sample performance is evaluated using leave-one-year-out validation. Each calendar year is held out once. The model is estimated on the remaining years, and fit is evaluated in the excluded year. In-sample performance is reported using R^2 , adjusted R^2 , RMSE, and MAE. LOYO performance is reported by holdout year and summarized using mean R^2 , median R^2 , pooled R^2 , mean RMSE, and mean correlation.